J. Indian Chem. Soc.,
Vol. 96, January 2019, pp. 126-130

Visible light activity of sulfur doped TiO_2 nanoparticles prepared by one step process

S. Arunmetha* and R. Jayavel

Crystal Growth Centre, Anna University, Chennai-600 025, India

E-mail: sarunmetha@gmail.com

Manuscript received online 02 September 2018, accepted 10 October 2018

The present research work emphasizes a new approach to prepare sulfur doped TiO_2 nanoparticles by one step chemical process. The main intent of this work is to reduce the demerits of sulfur (S) doped TiO_2 nanoparticles preparation, in requisites of the simple, cost effective, and mass preparation parameters. The physicochemical properties of undoped and doped TiO_2 were emphasized by XRD, FTIR, UV-Vis, PL, SEM with EDS and TEM analysis. The observed results shows the smaller crystallite size (10–12 nm) with spherical morphology of individual grains based on the XRD, SEM and TEM analysis results. From the UV-Visible and PL analyses, it observed that the S doped TiO_2 has been improved the UV and Visible absorption. The optimized results were exhibits sulfur doping escalating the photogenerated electrons and holes during the photocatalytic reaction. The obtained nanoparticles can be utilized in photovoltaic devices as photoanode material.

Keywords: Sulfur doped TiO_2, visible light active, single step process, photocatalytic.

Introduction

Titanium dioxide, also known as titanium(IV) oxide or titania (TiO_2), is a naturally occurring ninth most abundant oxide of titanium component. Since, this research work was commercial initiative in the early twentieth century. The structure of rutile and anatase can be described as tetragonal while brookite structure is depicted as orthorhombic[1]. Different synthesis methods are explored and developed for the preparation of TiO_2 nanoparticles including sol-gel[2], sonication[3], hydrothermal[4], ball mill[5] and spray pyrolysis[6].

Recent years a surge of invest in tuning the optical properties of TiO_2 nanoparticles for wide range of applications. The doping of sulfur in TiO_2 materials can enhance the absorption towards the visible spectrum during the photocatalytic activity. While analyzing this concept, we found that the surface modification of TiO_2 under visible light is significant. The chemical composition of TiO_2 can be changed by doping of metal (Fe, Ce, Cu, Zr, V, Mo etc.) and non-metal (C, N, S, F, B etc.)[7,8] components enhance optical as well as catalytic properties. It is require tremendous usage of material in energy crises via solar energy based on photovoltaic, water splitting, hydrogen preparation, and storage devices[9].

The non-metal ions doping with TiO_2 reduces the band gap value and form density of states. The sulfur doped TiO_2 (S-TiO_2) can be achieved through processes such as sol-gel, solvothermal, high temperature reactions, and hydrothermal[10]. The main aim of this work is to reduce the demerits of S-TiO_2 nanoparticles synthesis via simple, cost effective, and mass preparation parameters. The different characterisation techniques are used to analyze the effect of sulfur alteration in TiO_2 nanoparticles.

Experimental

Chemical reagents sulfuric acid (H_2SO_4: 98%, Merck) and titanium(IV) isopropoxide ($Ti(OCH(CH_3)_2)_4$): 99%, Merck) were purchased and used for the preparation of nanoparticles without any additional purification. The double distilled (DD) water was also used for the process of preparation. In this preparation method 7 *M* of H_2SO_4 (120 mL) was placed in a beaker. In this solution, 30 mL of titanium isopropoxide [$Ti(OPr)_4$] was added (drop wise) under magnetic stirring for 3 h. After the mixture was aged overnight to obtain the gel, it was then dried at 353 K for about 12 h in a hot air oven. The final S doped TiO_2 nanoparticles were obtained once the mixture was ground to a fine powder, and then calcined at 673 K for 3 h in a muffle furnace under air atmosphere at a heating rate of 278 K per minute. The un-doped TiO_2

nanoparticles were synthesized using the same chemical precursor and procedure barring the use of 120 mL of DD water instead of H_2SO_4 solution.

Results and discussion

Fig. 1 shows the XRD pattern of the samples S-doped and pure TiO_2 nanoparticles. The absorbed XRD patterns for two samples are compared with the JCPDS (JCPDS card: 21-1272, 1999) and it coordinated well with the reported phase of anatase TiO_2, which indicate a crystalline nature with mainly anatase structure of samples. It shows a major peaks A (101), A (004), A (200), A (105), A (204), A (220), and A (215) dominated in two samples. The other phases of TiO_2 possess a lower electron transport capability than the anatase phase of TiO_2, which is responsible for higher photovoltaic performance[11]. The average crystalline dimension along with the crystal plane (101) at $2\theta = 25.5°$ has been approximated from the full width half maximum of the diffraction peaks using Scherer equation for (101) plane[11], by analyzing the results of XRD pattern. The average crystallite sizes are found to be 10 nm and 12 nm for S-doped and pure TiO_2 samples respectively.

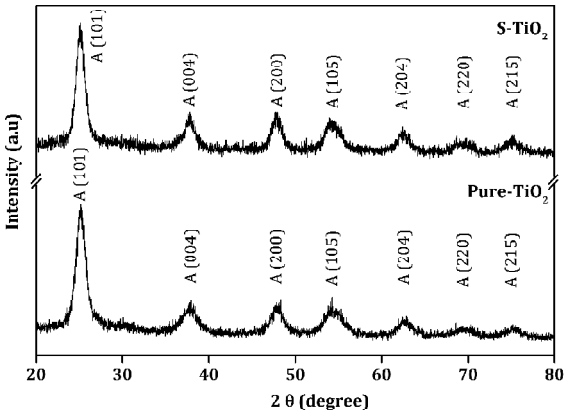

Fig. 1. XRD patterns of prepared S doped and pure TiO_2 nanoparticles.

The FTIR spectral assignments of the sample are shown in Fig. 2. The stretching vibration of Ti-O-Ti and Ti-O bonds is liable for the broad strong and similar peaks for two samples the range between 400 and 700 cm^{-1}. It is exhibits the existence of TiO_2 molecules in the sample[12,13]. When undoped TiO_2 sample is compared with S-doped samples, an additional absorbance peaks around 1120 cm^{-1} related to the symmetric stretching vibration of sulfate are noticed[14]. In

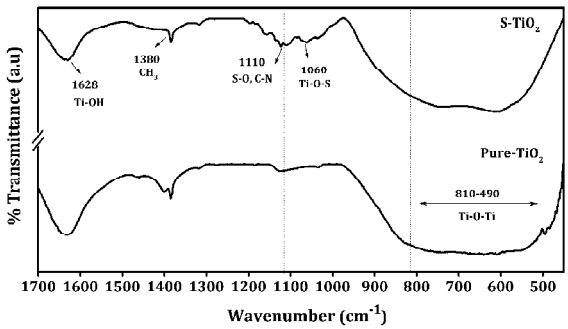

Fig. 2. FTIR spectra of prepared S doped and pure TiO_2 nanoparticles.

detail, the peaks observed at 1120 cm^{-1} correspond to the physically absorbed SO_2. Moreover, the distinctive peaks of the Ti-O-S bonds are not seen in the undoped TiO_2 sample. The same absorbance peak in the two samples corresponding to the hydroxyl groups and surface adsorbed water molecules O-H bending vibration[13].

The elemental compositions of the samples are confirmed by the EDS spectroscopy, as given in Fig. 3 and Table 1. The doped sample yields 96 wt.% TiO_2 and 3 wt.% of sulfur whereas undoped samples yield 99 wt.% of TiO_2. The observed results are reveal that sulfur doped in sample. The same kind of results is observed from XRF analysis as shown in Table 1. The FESEM images (Fig. 3) of the samples shows a weakly agglomerated spherical nanoparticles and its size ranges from several tens to hundred nanometres. The TEM images further confirms the spherical morphology as shown

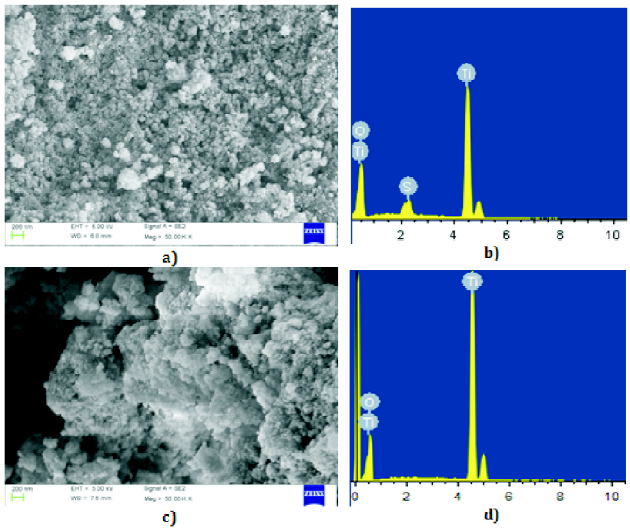

Fig. 3. FESEM image of prepared S doped (a, b) and pure (c, d) TiO_2 nanoparticles with EDS spectra.

Table 1. EDX and XRF analysis of TiO_2 nanoparticles

Prepared samples	EDX analysis		XRF analysis	
	Composition	Mass (%)	Composition	Weight (%)
S-TiO_2	TiO_2	96.43	TiO_2	99
	S	02.87		
Pure-TiO_2	TiO_2	99.12	TiO_2	99

in the FESEM images. The selected area diffraction (SAED) patterns are indexed as crystalline nature. The observed SAED pattern well matched with the XRD (Fig. 3) pattern.

The band gap energy of TiO_2 nanoparticles were calculated using measured optical absorption spectra values. Fig. 5 gives the diffused scattering UV-Vis spectra for TiO_2 nanoparticles. The band gap energy was calculated according to Max Planck's energy equation (eq. (1)). The onset wavelength (λ) was measured by extrapolating the absorption edge on the energy axis. For S-TiO_2 nanoparticles shows an onset of absorption λ_{os} = 390 nm, where as pure TiO_2 nanoparticles λ_{os} = 418 nm. Meanwhile the band gap values 3.17 eV and 2.96 eV respectively for doped and pure samples (Table 2). The nature of the band gap either an indirect or direct transition was established by following power expression for the variation of the absorption coefficient (α) with energy was examined and determined from the eq. (1).

$$\alpha = (2.303\times10^{3})(A)/l \quad (1)$$

where A is measured absorption and l is the optical path length (l) (1 cm).

$$(\alpha h\nu)^{n} = K_i(h\nu - E_g) \quad (2)$$

$$(\alpha h\nu)^{1/2} = K_d(h\nu - E_g) \quad (3)$$

where, K_i and K_d is the absorption constant for an indirect and direct transitions, $h\nu$ is absorption energy and E_g is the band gap energy.

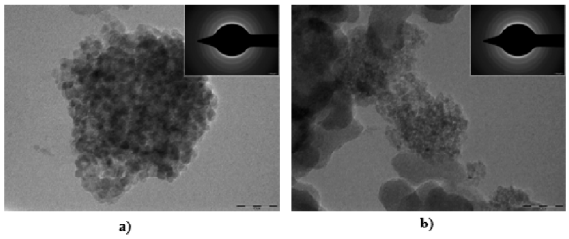

Fig. 4. TEM image of prepared S doped (a) and pure (b) TiO_2 nanoparticles with SAED.

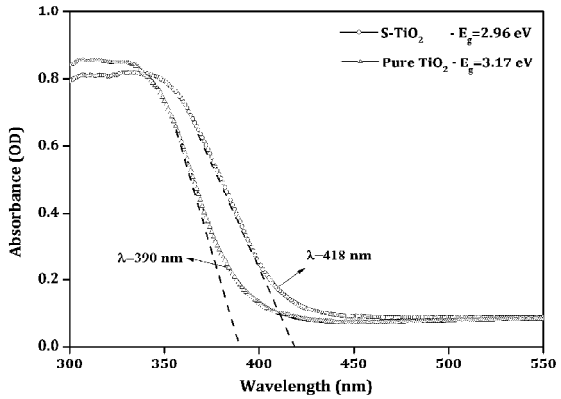

Fig. 5. UV-Visible spectra of prepared S doped and pure TiO_2 nanoparticles.

Table 2. Band gap energy of the as-prepared TiO_2 nanoparticles

Prepared samples	Band gap energy, E_g (eV) Calculation method		
	Max Planck's energy	Indirect transition	Direct transition
S-TiO_2	2.96	2.90	3.02
Pure-TiO_2	3.17	3.05	3.21

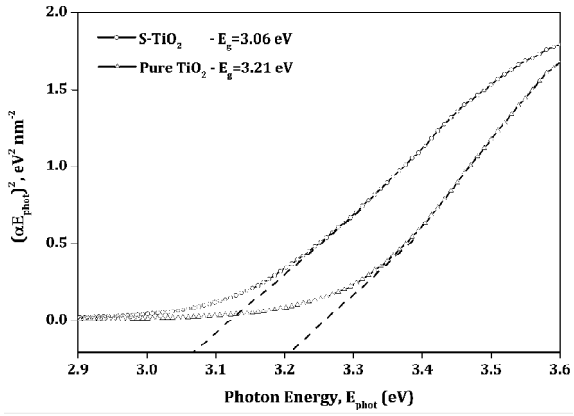

Fig. 6. Plot of $\alpha^{1/2}$ versus E_{phot} for indirect transition.

The absorption data were fitted to indirect band gap transition eq. (2) and direct band gap transition eq. (3). The Fig. 8 shows the $\alpha^{1/2}$ versus E_{phot} plot for an indirect transition and Fig. 7 shows the $(\alpha E_{phot})^2$ versus E_{phot} for a direct transition. In this absorption coefficient (α) is calculated using eq. (1) and E_{phot} is calculated. In Fig. 8 the value of E_{phot}

extrapolated to $\alpha = 0$ gives an absorption energy, which corresponds to a band gap E_g. The indirect fit plot yield band gap values of 2.90 eV and 3.05 eV respectively for S-TiO_2 and pure TiO_2 nanoparticles. The result in values of E_g estimated from the Fig. 7, the $\alpha = 0$ extrapolation as in the direct band gap values are 3.02 eV for S-TiO_2 and 3.21 eV for pure TiO_2 nanoparticles.

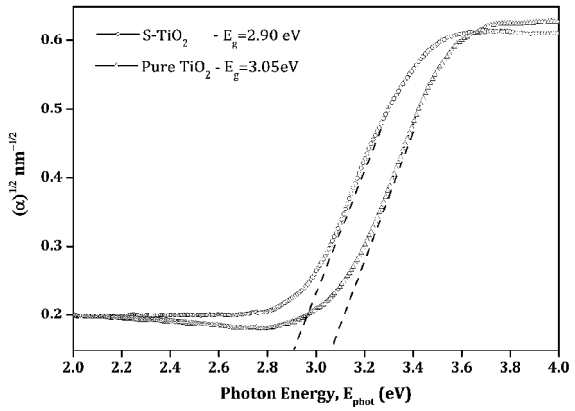

Fig. 7. Plot of $(\alpha E_{phot})^2$ versus E_{phot} for direct transition.

As tabulated in Table 2, it is interfered that the direct transitions plots are more appropriate than the indirect one when compared to the bandgap value determined using Max Plank energy equation. There is a shift in absorption peak from UV to visible when it is from pure to doped TiO_2 nanoparticles. It is occur due to transfer of charge from the valence band to conduction band. The lower band gap energy (2.96 –3.0 eV) is obtained for S-TiO_2 samples when compared to pure-TiO_2 samples band gap energy (3.17–3.2 eV).

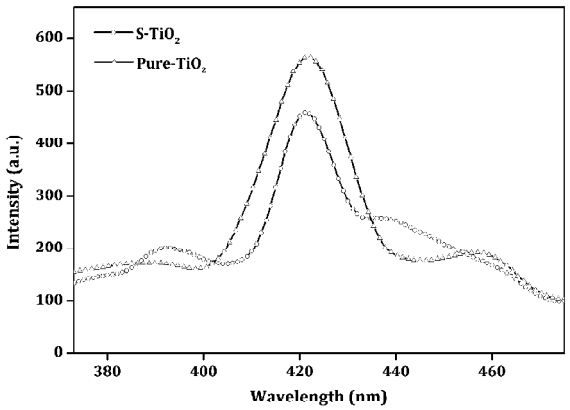

Fig. 8. PL emission spectra of prepared S doped and pure TiO_2 nanoparticles.

Fig. 8 shows PL spectra with similar curve shape and the position of the luminescence bands are associated to the crystalline structure and oxygen vacancies of the samples. A slight blue shift in the band intensity of the samples S-TiO_2 samples with respect to undoped TiO_2 sample[15], it is seen due to the influence of the sulfur ions. The result confirms that the existence of oxygen vacancies in the sample is provided due to the decrease in the intensity of the band and excitation wavelength. Oxygen vacancies are created owing to the non-metal doped (sulfur) in the samples[16].

Conclusions

A simple approach was employed to prepare S-TiO_2 nanoparticles via a one step sol-gel process. The prepared particles was characterised using XRD, FTIR, SEM with EDS, TEM, UV-Vis and PL analysis. The S-TiO_2 particles show the more absorption in UV as well in visible region when compared to pure TiO_2. The enhancement in the UV-Vis region was mainly attributed to the sulfur dopant, which enhanced the visible light adsorption as a result of their light harvesting property in the visible range due to the surface Plasmon effect. In addition, the presence of the sulfur dopant helps to reduce the band gap and shift the optical absorbance toward the visible region. The S-TiO_2 nanoparticles have continued to be highly active photocatalytic and photovoltaic applications.

Acknowledgements

Authors are grateful to the Science and Engineering Research Board (SERB), New Delhi, for giving National Post-Doctoral Fellowship (N-PDF) to carry out this research work (Sanction no. PDF/2016/000725 dt. 25.10.2016).

References

1. I. Banerjee, S. Karmakar, N. Kulkarni, A. Nawale, V. L. Mathe, A. K. Das and S. V. Bhoraskar, *Nanoparticle Res.*, 2010, **12**, 581.
2. S. Sahni, S. B. Reddy and B. S. Murty, *Mat. Sci. Eng. A*, 2007, 452.
3. W. A. Daoud, J. H. Xin and G. K. H. Pang, *Amer. Ceramic Soc.*, 2005, 443.
4. M. Kang, S.-Y. Lee, C.-H. Chung, S. M. Cho, G. Y. Han, B.-W. Kim and K. J. Yoon, *Photochem. Photobio. A: Chem.*, 2001, **144**, 185.
5. X. H. Xia, Y. S. Luo, Z. Wang, Y. Liang, J. Fan, Z. J. Jia and Z. H. Chen, *Mat. Lett.*, 2007, **61**, 2571.

6. M. Farbod and M. Khademalrasool, *Powder Tech.*, 2011, **214**, 344.
7. K. Nagaveni, M. S. Hegde and G. Madras, *Phys. Chem. B*, 2004, **108**, 20204.
8. X. Chen and C. Burda, *J. Am. Chem. Soc.*, 2008, **130**, 5018.
9. F. Li, W. Liu, Y. Lai, F. Qin, L. Zou, K. Zhang and J. Li, *Alloys and Compounds*, 2017, **695**, 1743.
10. S. Arunmetha, V. Rajendran, M. Vinoth, A. Karthik, S. R. Srither, M. S. Panday, N. Nithyavathy, P. Manivasakan and M. Maaza, *Mat. Res. Exp.*, 2017, **4**, 35016.
11. N. G. Park, J. van de Lagemaat and A. J. Frank, *Phys. Chem. B*, 2000, **104**, 8989.
12. O. K. Simya, M. Selvam, A. Karthik and V. Rajendran, *Synthetic Metals*, 2014,**188**, 124.
13. M. Rashidzadeh, *Int. Photoenergy*, 2008.
14. K. Mohan Kumar, S. Godavarthi, T. V. K. Karthik, M. Mahendhiran, A. Hernandez-Eligio, N. Hernandez-Como, V. Agarwal and L. Martinez Gomez, *Mat. Lett.*, 2016, **183**, 211.
15. K. M. Rahulan, S. Ganesan and P. Aruna, *Adv. Nat. Sci. Nanosci. Nanotech.*, 2011, **2**, 025012.
16. S. Arunmetha, P. Manivasakan, A. Karthik, N. R. Dhinesh Babu, S. R. Srither and V. Rajendran, *Adv. Powder Tech.*, 2013, **24**, 972.